AGU PUBLICATIONS

JGR

Journal of Geophysical Research: Atmospheres

RESEARCH ARTICLE
10.1002/2013JD020485

Special Section:
Study of Houston Atmospheric Radical Precursors (SHARP)

Emission measurements of alkenes, alkanes, SO_2, and NO_2 from stationary sources in Southeast Texas over a 5 year period using SOF and mobile DOAS

John K. E. Johansson[1], Johan Mellqvist[1], Jerker Samuelsson[1], Brian Offerle[1], Barry Lefer[2], Bernhard Rappenglück[2], James Flynn[2], and Greg Yarwood[3]

[1]Department of Earth and Space Sciences, Chalmers University of Technology, Gothenburg, Sweden, [2]Department of Earth and Atmospheric Sciences, University of Houston, Houston, Texas, USA, [3]ENVIRON International Corporation, Novato, California, USA

Key Points:
- Total VOC, SO2 and NO2 emission fluxes are measured from industries in Houston
- Reported VOC emissions are typically underestimated by an order of magnitude
- Meteorological variations cannot alone explain VOC emission discrepancies

Correspondence to:
J. K. E. Johansson,
john.johansson@chalmers.se

Citation:
Johansson, J. K. E., J. Mellqvist, J. Samuelsson, B. Offerle, B. Lefer, B. Rappenglück, J. Flynn, and G. Yarwood (2014), Emission measurements of alkenes, alkanes, SO_2, and NO_2 from stationary sources in Southeast Texas over a 5 year period using SOF and mobile DOAS, *J. Geophys. Res. Atmos.*, *119*, 1973–1991, doi:10.1002/2013JD020485.

Received 1 JUL 2013
Accepted 27 DEC 2013
Accepted article online 4 JAN 2014
Published online 27 FEB 2014

Abstract A mobile platform for flux measurements of VOCs (alkanes and alkenes), SO_2, and NO_2 emissions using the Solar Occultation Flux (SOF) method and mobile differential optical absorption spectroscopy (DOAS) was used in four different studies to measure industrial emissions. The studies were carried out in several large conglomerates of oil refineries and petrochemical industries in Southeast and East Texas in 2006, 2009, 2011, and 2012. The measured alkane emissions from the Houston Ship Channel (HSC) have been fairly stable between 2006 and 2011, averaging about 11,500 kg/h, while the alkene emissions have shown greater variations. The ethene and propene emissions measured from the HSC were 1511 kg/h and 878 kg/h, respectively, in 2006, while dropping to roughly 600 kg/h for both species in 2009 and 2011. The results were compared to annual inventory emissions, showing that measured VOC emissions were typically 5–15 times higher, while for SO_2 and NO_2 the ratio was typically 0.5–2. AP-42 emission factors were used to estimate meteorological effects on alkane emissions from tanks, showing that these emissions may have been up to 35–45% higher during the studies than the annual average. A more focused study of alkene emissions from a petrochemical complex in Longview in 2012 identified two upset episodes, and the elevation of the total emissions during the measurement period due to the upsets was estimated to be approximately 20%. Both meteorological and upset effects were small compared to the factor of 5–15, suggesting that VOC emissions are systematically and substantially underestimated in current emission inventories.

1. Introduction

The Houston-Galveston-Brazoria area, which includes eight counties in the vicinity of Houston, Texas, is a nonattainment area for the 2008 National Ambient Air Quality Standard for ozone. Ground-level ozone is formed through a chemical process in the atmosphere, fueled by sunlight and emissions of volatile organic compounds (VOCs) and nitrogen oxides (NO_x). Many large metropolitan areas in the U.S. have trouble meeting ozone standards since urban areas generally have a high concentration of anthropogenic sources of VOCs and NO_x. However, the Houston area is special due to its high concentration of refineries and petrochemical industries. These industries are primarily associated with VOC emissions but also have a significant NO_x contribution.

Measurements during the 2000 TexAQS (Texas Air Quality Study) and the 2006 TexAQS II indicated that the best emission inventories available at the time significantly underestimate industrial VOC emissions in Houston [*Kleinman et al.*, 2002; *Karl et al.*, 2003; *Ryerson et al.*, 2003; *Wert et al.*, 2003; *Jobson et al.*, 2004; *De Gouw et al.*, 2009; *Parrish et al.*, 2009; *Mellqvist et al.*, 2010b; *Washenfelder et al.*, 2010]. Several studies also concluded that industrial VOC emissions contribute significantly to ozone formation [*Kleinman et al.*, 2002; *Ryerson et al.*, 2003; *Wert et al.*, 2003; *Jobson et al.*, 2004; *Gilman et al.*, 2009; *Kim et al.*, 2011].

Industries are required to report the emissions from their activities to the state governments according to guidelines from the United States Environmental Protection Agency (EPA). The industries typically estimate their emissions with emission factors calculated using methods and formulas described in *AP-42, Compilation of Air Pollutant Emission Factors* [*United States Environmental Protection Agency* (*USEPA*), 2013]. VOC emissions from refineries and petrochemical industries are typically dominated by evaporative losses from storage tanks and process equipment. NO_x and SO_2 emissions, on the other hand, primarily come from external

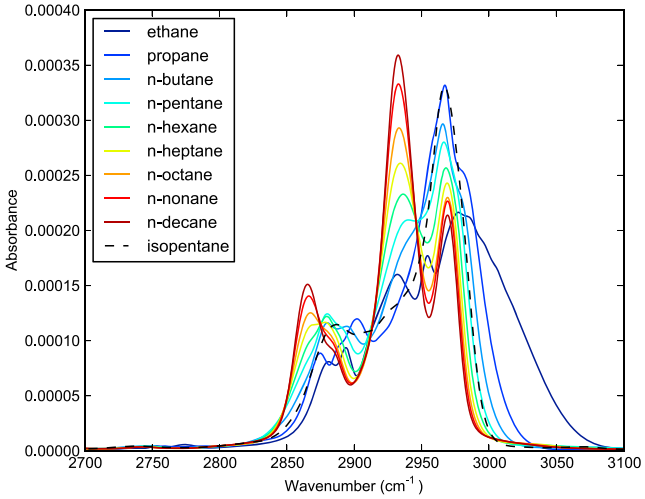

Figure 1. Absorbance spectra for 1 mg/m^2 of each of the *n*-alkanes from ethane to *n*-decane and isopentane degraded to 8 cm^{-1} spectral resolution.

combustion sources. This difference in types of emission sources makes VOC emission estimates inherently less reliable. External combustion is generally intentional and takes place in a limited number of places in a facility, often under controlled conditions with emissions released through flue gas channels which can be monitored to verify emission. Flares are an exception though. Estimates of SO_2 emissions from combustion are arguably even more reliable due to sulfur mass balance constraints; i.e., they are limited by the amount of sulfur in the burnt fuel. Evaporative losses of VOCs, on the other hand, can potentially occur in every unit in which petroleum products are stored, processed, or transported. Units that are malfunctioning, in need of maintenance, or irregularly operated can have drastically elevated emissions without giving any other indication. These types of irregular emissions can remain unnoticed if measurements of diffuse emissions are not made. Methods for quantitatively measuring these types of VOC emissions exist but are intrinsically more difficult due to the diffuse nature and the large number (tens of thousands) of potential sources. Estimates of VOC emissions from refineries and petrochemical industries are therefore rarely verified by quantitative measurements. Since reported total VOC emissions from a facility are typically a very small fraction (typically in the order of 0.01–0.02%) of its throughput, emissions would remain insignificant in any type of mass balance even if they were many times larger than reported.

In this paper we present measurements of VOCs, SO_2, and NO_2 from four campaigns in Southeast and East Texas carried out during 2006, 2009, 2011, and 2012. Additionally, a Solar Occultation Flux (SOF) spectral evaluation routine for alkanes is presented in detail and evaluated on the basis of its ability to quantify alkane mass columns in typical VOC mixtures from refineries. The measurement results are compared to emissions reported to the State of Texas Air Reporting System (STARS), and the representativeness of the results is discussed in relation to meteorological conditions, based on the use of the AP-42 emission factors.

2. Methods

All emission measurements presented in this article are based on the two methods, Solar Occultation Flux (SOF) and mobile DOAS (differential optical absorption spectroscopy). Both of them are based on the same principles for measuring total fluxes, instead of just concentrations, of industrial emission plumes. They take advantage of the ability of open path absorption spectroscopy methods to measure column concentrations. An emission flux is calculated from a series of column concentrations measured while traversing a plume crosswind together with some form of wind velocity measurement. The difference between the methods is mainly in the spectroscopy. SOF [*Mellqvist et al*., 2010b] is based on infrared measurements of direct sunlight, while mobile DOAS [*Galle et al*., 2002] is based on UV measurements of scattered sunlight.

2.1. Solar Occultation Flux

The Solar Occultation Flux method (SOF) is based on infrared measurements of direct sunlight from a mobile platform, typically a small truck, using a Fourier transform infrared (FTIR) spectrometer with a solar tracker.

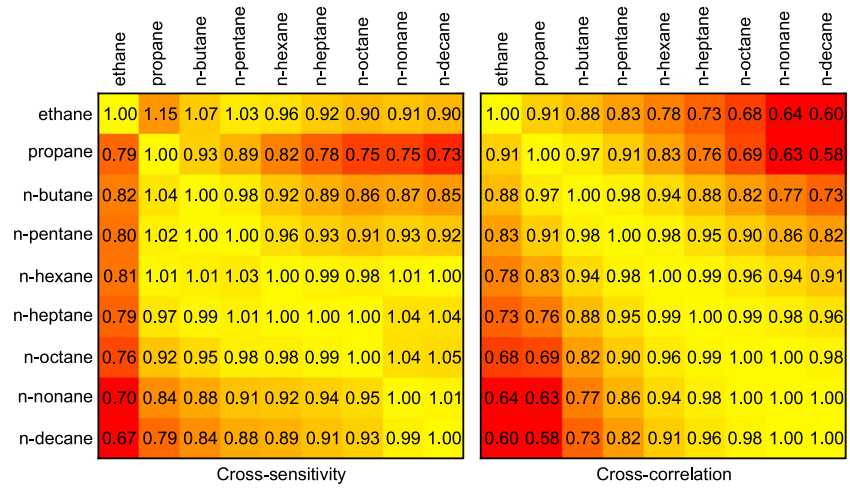

Figure 2. Cross sensitivity and cross correlation between each pair of *n*-alkanes from ethane to *n*-decane. The cross sensitivity is the ratio of the evaluated mass column to the true mass column, when evaluating the species on the *y* scale as the species on the *x* scale in a simple linear least squares retrieval in the interval 2700–3005 cm^{-1}. The cross correlation is the correlation coefficient between the two absorbance spectra in the same interval.

The solar tracker continuously guides the sunlight into the spectrometer as the truck moves and turns, and infrared spectra are recorded consecutively. These spectra are evaluated for absorption by molecular species in the industrial emission plume. A detailed description of the principles for SOF measurements and its application for measurements of ethene and propene is given in *Mellqvist et al*. [2010b].

In addition to ethene and propene, this study focuses on SOF measurements of alkanes. The evaluation of ethene and propene are based on narrow absorption lines in the interval 900–1000 cm^{-1} which are very specific to each species, while the alkane evaluation is based on a much broader absorption band in the region 2700–3000 cm^{-1}. This is called the C-H stretch band, since it corresponds to vibrational excitations of carbon-hydrogen bonds. Since C-H bonds are present in most VOCs, they typically have absorption features in this band. Figure 1 shows the absorbance spectra for all *n*-alkanes from ethane to decane downgraded to a spectral resolution of 8 cm^{-1}, which is typically used for these measurements. They are all fairly similar, and most of the variations are among the shorter alkanes, while the shape seems to almost converge the longer the carbon chain gets. Additionally, all alkanes have almost the same total absorption, i.e., the area under each absorbance spectra, for equal mass columns. These properties make it possible to approximate the combined absorption of any mix of alkanes fairly well with the combination of just a few of their absorbance spectra, and this combination will also approximate the total mass column of the alkane mix. This is important because the number of absorption spectra included in a spectral fitting routine has to be limited to avoid numerical instability, overfitting, and sensitivity to noise. To determine which absorption spectra to include in the evaluation, their similarities were quantified by pairwise calculation of cross sensitivity, i.e., how well the mass column of one alkane is approximated by a simple linear least squares fit to the absorbance spectrum of the other, and cross correlation. The cross sensitivity is a measure of how well a species approximates the mass column of another species in a spectral evaluation, while cross correlation is a measure of how good the spectral fit would be. In a spectral evaluation with several species included, absorption by another species is most likely to be approximated by the species it has high cross correlation with, since the spectral evaluation strives to optimize the spectral fit. The result of this is presented in Figure 2. This confirms the picture that the largest variations are among the shorter alkanes, while the longer ones are more similar to each other. For this reason it is more important to include the absorbance spectra of several shorter alkanes in the spectral fitting routine, while a single long alkane is sufficient to approximate the rest of them. This is also additionally motivated by the fact that gaseous emissions are typically dominated by shorter alkanes since they are more volatile. Accurate determination of alkane columns is further complicated by the presence of branched alkanes and cycloalkanes, which diverge slightly more in cross sensitivity from straight alkanes of similar carbon number. Isopentane is also included in Figure 1 as an example of this, showing that it is fairly similar in shape to straight alkanes but with somewhat lower total absorption, i.e., the area under the graph. However,

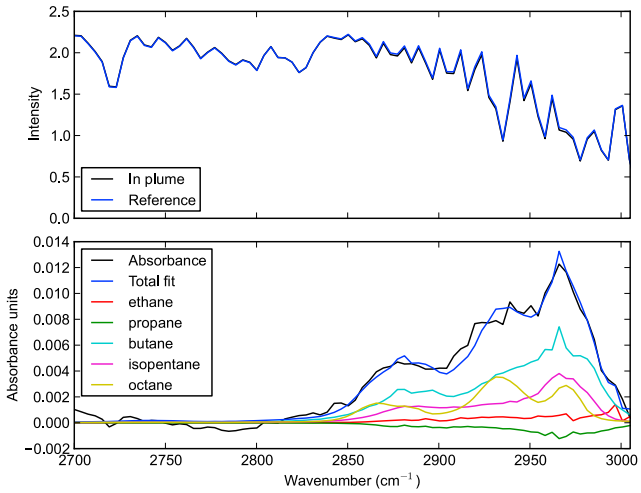

Figure 3. (top) SOF spectrum measured in a VOC plume and a reference spectrum measured outside of the plume. (bottom) Absorbance in the plume relative to the reference, fitted absorbance, and the fitted components of ethane, propane, butane, isopentane, and octane.

since the fraction of branched alkanes and cycloalkanes in VOC emissions from petroleum industries is typically low, the error of fitting them as straight alkanes is fairly limited.

A combination of ethane, propane, *n*-butane, isopentane, and *n*-octane was chosen to be included in the spectral fitting routine for the alkane measurements in this paper. The inclusion of isopentane was motivated by its relatively high abundance in VOC emissions compared to other branched alkanes and cycloalkanes. Absorption spectra for these species from the Pacific Northwest National Laboratories database [*Sharpe et al.*, 2004] were downgraded to 8 cm^{-1} resolution and were fitted by multivariate regression to the absorbance in the interval 2700–3005 cm^{-1}. Absorption spectra for water and methane, synthesized with line parameters from the HITRAN database [*Rothman et al.*, 2005], were also included in the fitting routine, which was performed in the QESOF software [*Kihlman*, 2005]. The total alkane mass column was calculated as the sum of the fitted mass columns of all the included alkanes. Figure 3 shows an example of a spectral fit and the alkane components fitted. The 8 cm^{-1} spectral resolution was empirically determined to be a good compromise between measurement signal-to-noise, sampling time, and sensitivity to spectral interference from other species.

In order to validate the accuracy of the alkane mass columns determined by this spectral fitting routine, data [*Texas Commission on Environmental Quality* (*TCEQ*), 2013] from an automated gas chromatograph in a Continuous Ambient Monitoring Station (CAMS), C169 located close to the Houston Ship Channel (HSC) (29.7062492°, −95.2611301°) and operated by TCEQ (Texas Commission on Environmental Quality), were used to approximate typical refinery VOC compositions in Houston. Data from September 2006, the time of the first measurement campaign, was filtered for hourly averages where wind speed was above 1.4 m/s and wind direction was in the interval 69°–87°. In these wind directions the emissions from refineries in the HSC should dominate the VOC concentrations measured at CAMS 169. Seven such instances were found during September 2006. For each of these instances an artificial solar spectrum was synthesized with absorption by different VOCs in the proportions measured by the auto-GC. These spectra were downgraded to the resolution of the spectral retrieval, 8 cm^{-1}, and evaluated by the spectral fitting routine described above. The evaluated alkane mass columns were then compared to that used for synthesizing the solar spectra. The results of this are presented in Table 1. The evaluated alkane mass overestimated the true alkane mass by 3–7%, which is small compared to the uncertainty in flux calculations due to wind speed uncertainty. This overestimation is due to a combination of the errors of fitting all alkanes to a finite set and the spectral interference from other VOCs with weaker absorption in the same region.

Methane is typically treated separately from other VOC emissions because it has much lower ozone formation potential. Fortunately, the alkane evaluation routine described above has low sensitivity to methane. Methane has absorption in this band but primarily in narrow lines. Because of the relatively high background concentration of methane, these lines are practically depleted of light after passing through the full atmospheric column. This is illustrated in Figure 4. Due to the nonlinearity of Beer-Lamberts law at such strong

Table 1. VOC Composition in the Plume Downwind of a Large Refinery Complex in the HSC During Seven Episodes in the 2006 Study as Measured by an Auto-GC at CAMS 169[a]

		Date and Time						
	Molar mass	2 Sep 2006, 19:00	4 Sep 2006, 17:00	9 Sep 2006, 21:00	9 Sep 2006, 22:00	20 Sep 2006, 11:00	20 Sep 2006, 12:00	26 Sep 2006, 16:00
Wind speed (m/s)		1.70	1.43	2.28	1.88	2.55	2.86	1.43
Wind direction (deg)		76	72	87	86	69	76	77
Units	g/mole	ppbv	ppbv	ppbv	ppbv	ppbv	ppbv	ppbv
Alkanes								
Ethane	30.1	17.93	2.59	3.46	4.59	10.51	7.52	3.64
Propane	44.1	20.20	1.23	1.71	2.22	9.40	4.84	2.09
n-Butane	58.1	12.85	1.14	0.87	0.58	8.74	4.97	1.07
i-Butane	58.1	4.87	0.37	0.68	0.60	3.84	2.41	1.03
cyc-Pentane	70.1	1.01	0.09	0.16	0.04	0.43	0.23	0.05
i-Pentane	72.2	16.07	1.35	1.43	0.47	6.69	4.17	0.74
n-Pentane	72.2	12.52	0.80	0.94	0.24	4.23	2.37	0.42
cyc-Hexane	84.2	2.17	0.09	0.14	0.04	0.49	0.24	0.04
2,2-Dimethylbutane	86.2	0.33	0.04	0.08	0.03	0.20	0.11	0.02
n-Hexane	86.2	2.40	0.18	0.48	0.14	1.21	0.71	0.19
3-me-Hexane	100.2	0.45	0.05	0.14	0.05	0.32	0.22	0.05
n-Heptane	100.2	0.65	0.05	0.13	0.04	0.33	0.21	0.04
n-Octane	114.2	0.31	0.04	0.09	0.02	0.19	0.11	0.03
i-Octane	114.2	0.36	0.10	0.18	0.08	0.58	0.24	0.08
n-Nonane	128.2	0.07	0.01	0.02	0.01	0.05	0.03	0.01
n-Decane	142.2	0.04	0.01	0.02	0.03	0.05	0.03	0.01
Alkenes								
Ethylene	28.0	4.16	0.46	0.75	0.50	1.96	1.51	0.66
Propylene	42.1	3.94	0.24	0.99	0.92	1.66	0.90	0.42
1,3-Butadiene	54.1	0.44	0.40	0.16	0.18	0.12	0.12	0.48
t-2-Butene	56.1	0.68	0.13	0.09	0.07	0.12	0.10	0.12
1-Butene	56.1	0.65	0.14	0.06	0.03	0.36	0.20	0.09
c-2-Butene	56.1	0.52	0.07	0.06	0.04	0.09	0.07	0.07
Isoprene	68.1	0.20	0.24	0.01	0.01	0.22	0.10	0.10
t-2-Pentene	70.1	0.69	0.04	0.07	0.02	0.08	0.05	0.02
1-Pentene	70.1	1.07	0.06	0.05	0.02	0.12	0.08	0.03
c-2-Pentene	70.1	0.32	0.02	0.04	0.01	0.04	0.03	0.01
Styrene	104.1	0.07	0.00	0.29	3.58	0.02	0.11	0.16
Aromatics								
Benzene	78.1	0.82	0.12	0.21	0.11	0.64	0.57	0.22
Toluene	92.1	2.40	0.26	0.49	0.27	0.70	0.54	0.41
m + *p*-Xylene	106.1	0.42	0.07	0.24	0.10	0.25	0.17	0.17
o-Xylene	106.1	0.13	0.02	0.10	0.10	0.10	0.08	0.06
Ethylbenzene	106.1	0.18	0.03	0.10	0.09	0.09	0.06	0.07
Mass fractions								
Alkanes		84.7%	76.4%	71.1%	44.0%	87.9%	85.3%	70.4%
Alkenes		9.4%	15.5%	15.5%	48.9%	6.6%	7.6%	16.3%
Aromatics		5.9%	8.1%	13.4%	7.0%	5.4%	7.1%	13.4%
Retrieved/true alkane mass		1.044	1.051	1.062	1.058	1.035	1.036	1.065

[a]The uncertainty of the alkane spectral retrieval has been estimated by applying it to solar spectra with absorption by VOCs added synthetically proportionally to the measured concentrations. The mass ratios between the evaluated alkane columns and the total alkane columns added synthetically are given at the bottom of the table. The mass fractions of alkanes, alkenes, and aromatics are also presented to give an overview of the composition.

absorption, the apparent absorption of additional methane at 8 cm^{-1} resolution is approximately a factor of 17 lower than it would be without the atmospheric methane background column. The absorption spectrum of methane is still included in the alkane spectral fitting routine but mainly to improve the spectral fit and not to quantify methane. Quantitative measurement of atmospheric methane using solar FTIR is possible but generally requires high-resolution measurements [*Angelbratt et al.*, 2011].

2.2. Mobile DOAS

For mobile DOAS measurements UV spectra of solar light scattered in the atmosphere are measured with a UV spectrometer, typically a Czerny-Turner spectrometer with a CCD detector. The spectrometer is typically connected

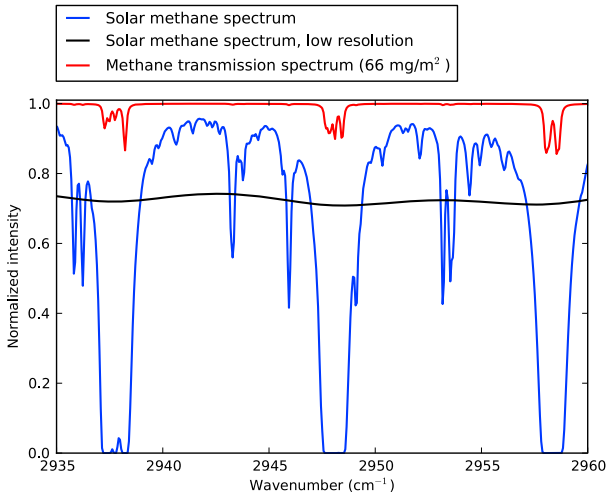

Figure 4. High-resolution solar spectrum (blue) after passing through the full atmospheric methane column and the same solar spectrum downgraded to a resolution of 8 cm^{-1} (black). Although not obvious from the low-resolution spectrum, the strong absorption lines are depleted of light.

with a light guide to a zenith-looking telescope. The principles for mobile DOAS measurements are described in detail by *Galle et al.* [2002], *Johansson et al.* [2008, 2009], *Rivera et al.* [2009, 2010], and *Johansson et al.* [2014] together with its application for measuring SO_2 and NO_2 in *Johansson et al.* [2008] and *Rivera et al.* [2009, 2010] as well as formaldehyde (HCHO) in *Johansson et al.* [2008, 2009], *Rivera et al.* [2010], and *Johansson et al.* [2014].

The measurements in 2009, 2011, and 2012 used a 303 mm focal length Czerny-Turner spectrometer (ANDOR Shamrock 303i) with a 1024 × 255 pixel, thermoelectrically cooled CCD detector (Newton DU920N-BU2) which was connected with a liquid light guide, 3 mm in diameter, to a zenith-looking quartz telescope with a 75 mm diameter and a 20 mrad field of view. The holographic grating used (1800 grooves/mm) together with a 300 μm entrance slit gave a 0.63 nm spectral resolution in the 309–351 nm wavelength region that the CCD was set to cover. The telescope was equipped with an optical band pass filter (Hoya), blocking wavelengths above 380 nm to reduce stray light in the spectrometer. This is a highly light-sensitive DOAS system originally developed for airborne measurements of ship emissions using downward looking DOAS [*Berg et al.*, 2012]. This was the same system and setup as in *Johansson et al.* [2014], and NO_2 was evaluated with the same spectral fitting routine as formaldehyde in that paper. This routine involved fitting cross sections for HCHO [*Cantrell et al.*, 1990], NO_2 [*Vandaele et al.*, 1998], O_3 [*Burrows et al.*, 1999], $(O_2)_2$ collision complex [*Hermans et al.*, 1999], a ring spectrum, and a polynomial of order 3 in the 324–350 nm spectral window. Wavelength calibration of the spectrometer was made with respect to the Fraunhofer lines present in all solar spectra. SO_2 was also evaluated from the same spectra using a 310–325 nm spectral window where SO_2 [*Bogumil et al.*, 2003], O_3 [*Burrows et al.*, 1999], a ring spectrum, and a polynomial of order 3 were fitted. Apart from spectral window and cross sections fitted, the two routines were identical. The QDOAS software [*Fayt*, 2011] was used for the wavelength calibration, degradation of cross sections, ring spectrum synthesis, and spectral fitting. Further details of the NO_2/HCHO evaluation routine can be found in *Johansson et al.* [2014]. During the 2006 study, a commercial mini-DOAS system was used instead of the one described above. This system collected less light and therefore required longer exposure times to achieve the same accuracy. The mobile DOAS results from this study was previously published in *Rivera et al.* [2010] together with a complete description of the system used.

2.3. Wind Measurements

Accurate wind information is of major importance for flux calculations for both SOF and mobile DOAS. Even though considerable effort is put into obtaining high-quality wind measurements, wind uncertainty is typically the largest error source for flux measurements. Measurements of wind height profiles throughout the boundary layer were taken during all four campaigns using GPS tracking radiosondes launched with helium balloons. Since the number of radiosonde launches on a given measurement day varied between five and zero, profiles derived from these launches were not available sufficiently close in time to the measurement

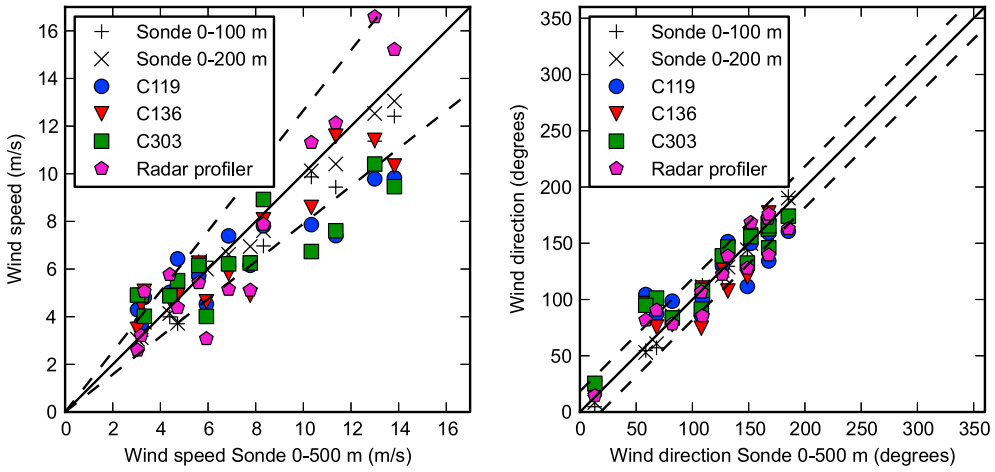

Figure 5. Comparison of different wind measurements in the Beaumont/Port Arthur area during the 2011 study. For each radiosonde launch the wind profile averages from ground up to 100 m and 200 m and simultaneous rescaled measurements at the ground stations C119, C136, and C303 and from a local radar profiler are plotted against the profile average from ground up to 500 m. The solid line represents perfect agreement, and the dashed lines show plus/minus the average of the standard deviations of the differences (relative differences for the wind speed) between the ground sources and the radiosonde profile average.

transects. Hence, the radiosonde data were complemented by wind measurements from local ground sites, mainly from the TCEQ-operated network of Continuous Ambient Monitoring Stations (CAMS) [*TCEQ*, 2013]. Ground wind speed data were normalized to radiosonde measurements to compensate for systematic wind speed differences as a function of height. Average winds over the first 500 m (350 m for the 2012 Longview study) of the wind profiles were used both for flux calculations and for normalization of ground wind data, as described in *Mellqvist et al*. [2010b]. Flux calculations were made using height profile averages when available sufficiently close in time to the measurement transect and normalized ground wind data for other cases. The variations between the different wind data sets were used to estimate the wind uncertainty. This is not a measurement uncertainty but rather the uncertainty due to the variation in the wind on the spatial and temporal scales that the wind measurements differ from the time and place of the column measurements. As an example, Figure 5 shows a comparison between height profile averages and simultaneous normalized ground wind measurements from CAMS sites in the Beaumont/Port Arthur area during the 2011 study. The estimated wind uncertainties based on these comparisons are presented in Table 2 for the different studies. The range of uncertainties given represents the 1σ variabilities of a number of ground wind stations compared to sonde profile averages. The estimated uncertainties were similar in most years, with the exception of 2012 in Longview, where especially the wind direction uncertainty was larger. This was suspected to have been at least partly caused by measurement errors in some of the ground wind measurements.

2.4. Emission Inventories

Emission inventory data were extracted from the STARS (State of Texas Air Reporting System) emission inventory for comparison to the measured emission rates. Emissions are reported to STARS by the industries on an annual basis and are typically based on calculations using emission factor formulas such as found in *AP-42, Compilation of Air Pollutant Emission Factors* [*USEPA*, 2013]. Data for 2006, 2009, and 2011 was extracted, and total emissions of the species of interest were computed as the sum of all point source emissions within each studied area. Emission inventories were not yet available for 2012. Speciation in the emission inventories did not perfectly match the speciation of the measurements. For comparison with the SOF alkane measurements, all emissions speciated as either alkanes or alcohols were added, as well as unspeciated VOCs and vaguely speciated VOCs, such as "crude oil" and "naphtha." Alcohols were included since they typically

Table 2. Wind Speed and Wind Direction Uncertainties for the Four Studies as Estimated From the Variation Between Sonde Profile Averages and Normalized Ground Wind Measurements

Year	Wind Speed Uncertainty	Wind Direction Uncertainty
2006	15–27%	11–33°
2009	11–29%	10–26°
2011	16–30%	11–23°
2012	25–34%	30–34°

Table 3. Total Number of Sites and Sources and Total Reported Average Emissions in the Emission Inventories for Harris County for All Measured Species and for the Years of the Studies

	Number of Sites			Number of Sources			Total Emissions (kg/h)		
Species	2006	2009	2011	2006	2009	2011	2006	2009	2011
Alkanes	261	262	266	10,052	8,398	8,822	1,597	1,224	1,293
Ethene	49	41	51	1,055	798	830	123	104	88
Propene	50	46	53	1,148	844	853	179	102	92
NO_x	228	234	240	2,449	2,255	2,331	3,241	1,877	1,664
SO_2	203	207	210	2,192	1,957	2,011	2,730	2,004	1,256

have absorption cross sections similar in shape and strength to alkanes in the C-H stretch spectral region. The unspeciated and vaguely speciated VOCs were included since they are probably dominated by alkanes in general but may contain some species that the alkane measurements are not sensitive to. NO_x emissions are reported to the inventories, while only NO_2 is measured with mobile DOAS. According to airborne measurement carried out in parallel to the SOF measurements during the 2006 study [*Rivera et al*., 2010], the typical NO_2/NO_x ratio was 0.75, which suggests that measured NO_2 emissions should be expected to be on average 25% lower than the reported emissions. The measured emissions of ethene, propene, and SO_2 were all possible to compare directly to the equivalent inventory species. Table 3 shows the total number of industrial sites and point sources within those sites reporting emissions of the species of interest to the inventories for Harris County, which contains all of the HSC and parts of Mont Belvieu, in 2006, 2009, and 2011. Alkane emissions (including alcohols and unspeciated VOC) are the most common, and almost every site reports something in this category, while ethene and propene are significantly less common. The number of point sources has stayed relatively constant, although there seems to have been a noticeable dip from 2006 to 2009. To what extent this represents changes in operations, as opposed to changes in reporting procedures, is not known.

The emissions are reported on an annual basis so even when converted to kg/h they should be thought of as annual average emissions. Since there can be large variations in emissions from a source within a year, instantaneous emissions cannot be expected to always match the annual average emissions. However, since each area contains a large number of sources in several independently operated facilities and measurements have been performed on multiple days and in different years, the measured emission should at least be expected to be roughly the same as the reported annual average emissions on average.

3. Results

The measurement results in this article were aggregated from four different studies of industrial emissions performed in Southeast and East Texas in the period 2006–2012. A map of the region is shown in Figure 6. The first study was a part of the Second Texas Air Quality Study (TexAQS II) [*Parrish et al*., 2009], and measurements lasted from August to September 2006. This study tried to cover as many refinery and petrochemical industry areas in the Greater Houston area as possible. As a result, the total number of measurements for each area was fairly low. An example of an alkane measurement series from this study is shown in Figure 7. This measurement was performed on 25 September 2006 in Houston Ship Channel, and separate plumes from a large number of facilities can easily be distinguished in the northerly wind. The second study was a part of the Study of Houston Atmospheric Radical Precursors [*Lefer*, 2009], and measurements lasted from April to June 2009. In this study, the measurements were focused on three areas: the HSC, Mont Belvieu, and Texas City. This allowed for a larger number of measurements, spread over more days, to be collected. Figure 8 shows an example of a combined alkane and alkene measurement series from this study. This measurement was performed in Mont Belvieu on 5 June 2009, and three separate plumes are detected. The simultaneous measurements of alkane, ethene, and propene suggest that they are only partly coemitted, and especially propene seems to have a separate source. The third study, lasting from April to May 2011, was a stand-alone field study covering the same areas as in 2009, as well as the Beaumont/Port Arthur area. A single day of measurements was also conducted at a petrochemical complex in Longview. An example of an alkane measurement series from this study is shown in Figure 9. This measurement was performed on 3 May 2011 and covered a number of the largest alkane emission sources in the Beaumont/Port Arthur area but not all of them. The fourth study was performed during May 2012 and was focused entirely on the

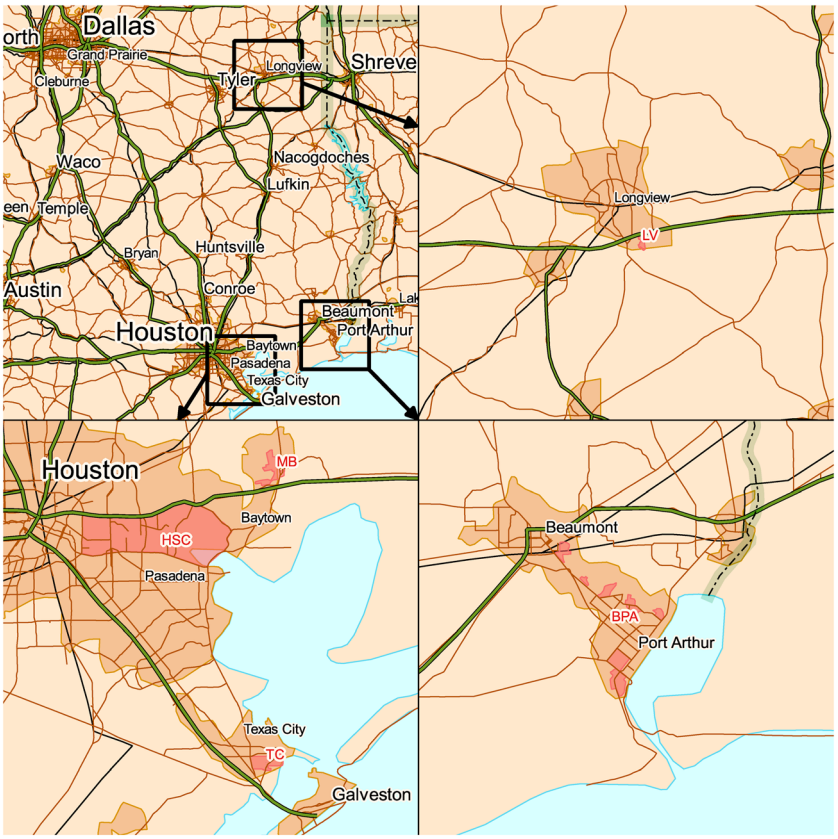

Figure 6. Map of Southeastern and Eastern Texas with zoomed in boxes around the areas studied. The areas are marked in red and denoted by their abbreviated names.

petrochemical complex in Longview. This allowed for a comprehensive set of measurements to be collected, giving a clearer picture of day-to-day variations. Figure 10 shows an example of a combined alkene and NO_2 measurement series from this study. This measurement was performed at the petrochemical complex on 7 May 2012. The measurement series for ethene and propene are closely correlated, but there is a clear spatial

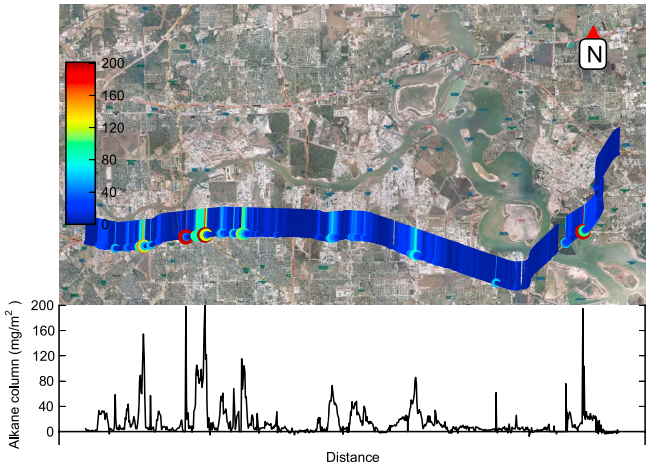

Figure 7. Alkane measurement transect covering all of the Houston Ship Channel (HSC) performed on 25 September 2006. Each measurement is indicated on the map with a circle and a line. The size and color of the circle indicates the magnitude of the alkane column measured, and the line indicates the direction the wind is blowing from. Below the map is a plot of the alkane column as a function of crosswind distance. This transect provided one alkane flux measurement for the HSC area.

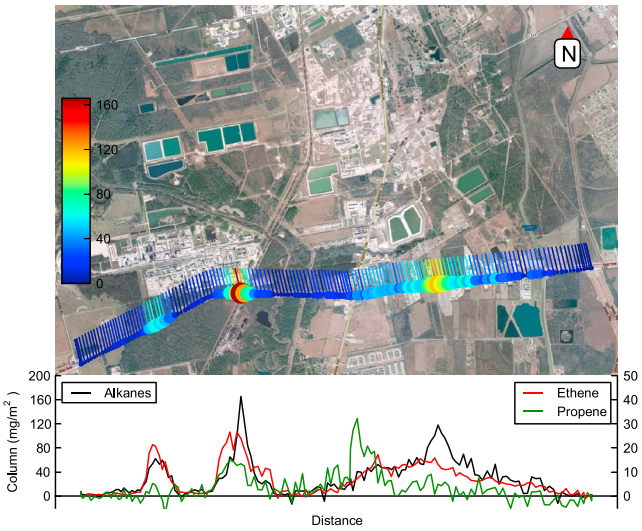

Figure 8. Measurement transect of alkanes, ethene, and propene covering all of Mont Belvieu performed on 5 June 2009. Each measurement is indicated on the map with a circle and a line. The size and color of the circle indicates the magnitude of the alkane column measured, and the line indicates the direction the wind is blowing from. Below the map is a plot of the columns of all species as a function of crosswind distance. This transect provided one flux measurement each for alkanes, ethene, and propene from Mont Belvieu.

separation between them and the NO_2 plume. However, this is most likely primarily caused by the different measurement angles of SOF and mobile DOAS. Ethene and propene are measured with SOF, which measures along the path of the direct sunlight, while NO_2 is measured with mobile DOAS, which measures in the zenith direction. This measurement was made in the morning when the sun was fairly low and in the east, which makes the alkene plume appear further to the west. Detailed results from all four studies are presented in *Mellqvist et al.* [2010b, 2007, 2010a] and *Johansson et al.* [2011, 2012].

The measurement results from all these studies have been aggregated to give an overview and enable comparison over time and between the different areas. These aggregated results are presented in Table 4

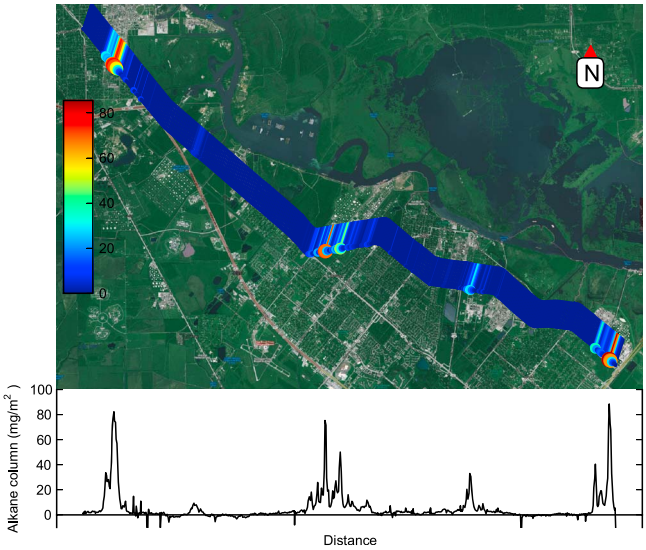

Figure 9. Alkane measurement transect covering a number of industries in the Beaumont/Port Arthur area performed on 3 May 2011. Each measurement is indicated on the map with a circle and a line. The size and color of the circle indicates the magnitude of the alkane column measured, and the line indicates the direction the wind is blowing from. Below the map is a plot of the alkane column as a function of crosswind distance. This transect provided one alkane flux measurement each for five subareas in Beaumont/Port Arthur.

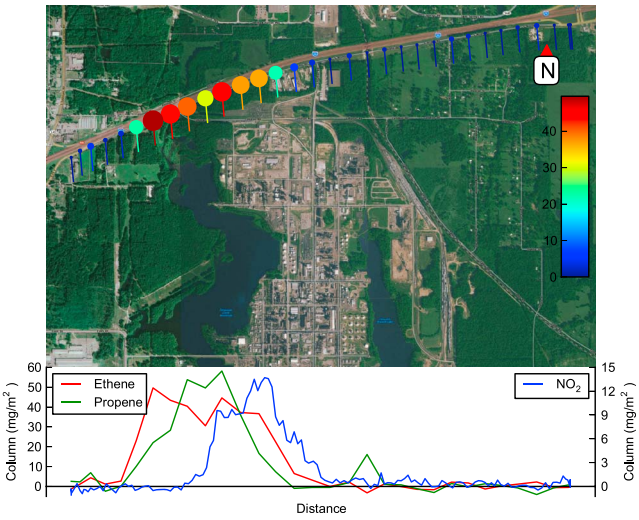

Figure 10. Measurement transect of ethene, propene, and NO_2 covering the petrochemical complex in Longview performed on 7 May 2012. Each measurement is indicated on the map with a circle and a line. The size and color of the circle indicates the magnitude of the ethene column measured, and the line indicates the direction the wind is blowing from. Below the map is a plot of the columns of all species as a function of crosswind distance. This transect provided a flux measurement each for ethene, propene, and NO_2 from Longview.

together with annual average emissions reported to the emission inventories for the corresponding areas. For each area, species and year, the table shows the total number of measurements, mean and standard deviation of the emission flux measured, and the reported annual average emission. In some cases, total emissions for an area was calculated as a sum of emissions from subareas and the number of flux measurements were not the same for all subareas. For these cases, mean emissions from the subareas were summed, standard deviations were root-sum-squared, and the number of total flux measurements is given as a range from the lowest number of measurements on a subarea to the highest. Reported emissions are the sum of the annual routine emissions for all point sources within an area, converted to average hourly emissions.

Many emissions seem to have been quite stable over the years. The mean total alkane emissions from the HSC have been within ±10% of 11,500 kg/h for all three studies. At the same time there are some large differences from year to year. The total propene emissions from the HSC, for example, were approximately 1500 kg/h in 2006 but dropped to roughly 600 kg/h in 2009 and 2011. However, as described in more detail in *Mellqvist et al*. [2010b], the variability in the propene emissions measured from the HSC in 2006 was exceptionally large, indicating temporary upset emissions. Despite some significant variations from year to year and from area to area, there is a clear pattern of measured VOC emissions (alkanes, ethene, and propene) exceeding reported emissions with almost an order of magnitude on average, while no similar pattern exists for SO_2 and NO_2. This pattern is highlighted in Figure 11, where the ratios between measured emissions and reported annual average emissions have been plotted for each year, species, and area. Reported emissions for 2011 were used for the 2012 ratios, since 2012 data were not yet available. Most ratios for SO_2 and NO_2 emissions are gathered fairly close to 1, while the ratios for alkanes, ethene, and propene are mostly within the interval of 5–10. There are of course differences between the areas and the years, but they are generally dwarfed by the difference between the species. The most striking exceptions to the overall pattern are the SO_2 emissions from Texas City. The reported SO_2 emissions from Texas City have steadily declined during the period of these studies, but no such decrease has been observed in the measurements. Instead, the measured mean emissions increased from 2009 to 2011, giving a measured to reported ratio of almost 12 in 2011. However, all SO_2 measurements in Texas City in 2011 were performed during a single day, which makes this comparison very sensitive to short-term variations. The unusually large discrepancy in 2011 SO_2 emissions from Texas City might be attributable to large nonroutine emissions during that single day. A large proportion of reported SO_2 emissions in Texas City are attributed to flares, which might have significant variability. Measurement with Multi-Axis DOAS [*Stutz et al*., 2011] were performed in parallel with the mobile DOAS measurements during the 2009 study and estimated the average SO_2 emissions during the period to be 510 kg/h, approximately halfway between the mobile DOAS result and the reported annual emissions.

Journal of Geophysical Research: Atmospheres

10.1002/2013JD020485

Table 4. Summary of All Total Flux Measurements for Each Area, Species, and Year[a]

		2006				2009				2011				2012			
Area	Species	*N*	Mean	Std	EI	*N*	Mean	Std	EI	*N*	Mean	Std	EI	*N*	Mean	Std	EI
Houston Ship Channel	Ethene	4	878	152	63	6	614	284	67	4–14	612	168	53	-	-	-	-
	Propene	3	1,511	529	149	4	642	108	70	1–9	563[b]	294	63	-	-	-	-
	Alkanes	3	12,276	3,491	1,208	3	10,522	2,032	814	5	11,569	2,598	894	-	-	-	-
	SO_2	3	2,277	1,056	2,570	10–23	3,364	821	1,784	18–25	2,329	466	1,228	-	-	-	-
	NO_2	9	2,460	885	2,303	-	-	-	-	5–16	1,830	330	1,103	-	-	-	-
Mont Belvieu	Ethene	6	443	139	82	23	444	174	59	6–9	545	284	47	-	-	-	-
	Propene	3	489	231	37	17	303	189	25	1	58[b]	-	25	-	-	-	-
	Alkanes	1	874	-	177	13	1,575	704	221	3	1,319	280	127	-	-	-	-
	NO_2	-	-	-	-	2–35	168	39	174	2	305	29	155	-	-	-	-
Texas City	Ethene	3	83	12	7	11	122	41	4	7–9	177	48	2	-	-	-	-
	Propene	ND	ND	ND	9	3	54	22	7	5	56[b]	9	6	-	-	-	-
	Alkanes	6	3,010	572	447	12	2,422	288	288	7	2,342	805	242	-	-	-	-
	SO_2	-	-	-	-	17–37	834	298	297	25–26	1,285	428	109	-	-	-	-
	NO_2	11	460	150	452	10	283	30	351	15–16	492	71	352	-	-	-	-
Beaumont and Port Arthur	Ethene	-	-	-	-	-	-	-	-	4–7	178	35	18	-	-	-	-
	Propene	-	-	-	-	-	-	-	-	1–5	53[b]	6	18	-	-	-	-
	Alkanes	-	-	-	-	-	-	-	-	1–12	7,413	1,448	407	-	-	-	-
	SO_2	-	-	-	-	-	-	-	-	3–22	1,612	447	2,377	-	-	-	-
	NO_2	-	-	-	-	-	-	-	-	3–18	1,422	268	965	-	-	-	-
Longview	Ethene	-	-	-	-	-	-	-	-	9	452	191	127	67	249	130	-
	Propene	-	-	-	-	-	-	-	-	8	282	59	32	60	211	122	-
	NO_2	-	-	-	-	-	-	-	-	4	176	51	231	92	118	33	-

[a]The table gives the number of measurements (N), the mean and standard deviation of the measured fluxes (Mean and Std), and the annual average emissions reported to the emission inventories (EI). All numbers are in kg/h except N, the number of measurements. A range given for N indicates that the mean emissions were calculated as the sum of the mean emissions from a number of subareas. N is the range of the number of measurements for each subarea. The standard deviation was calculated as the root-sum-square of the standard deviations of the subareas for these cases.

[b]Instrumental problems during parts of the 2011 campaign resulted in fewer propene measurements with larger uncertainty.

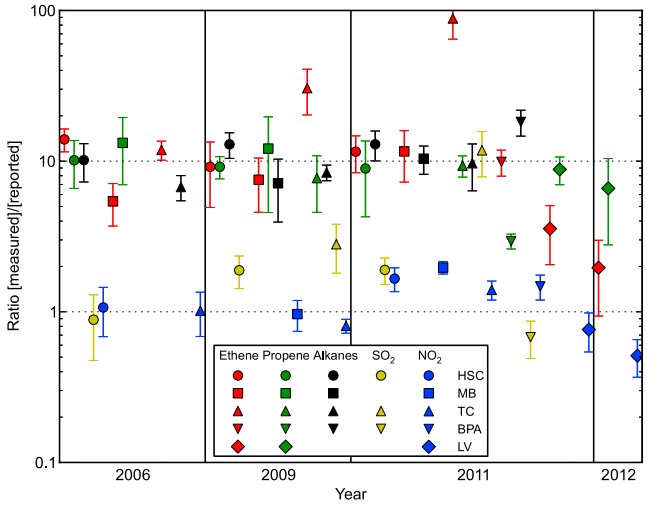

Figure 11. Ratios of emissions measured with SOF and mobile DOAS to annual average emissions reported to State of Texas Air Reporting System (STARS) for each year, species, and area. The markers indicate the ratio of the mean of all flux measurements to the reported emissions, while the error bars indicate ratio of the mean plus/minus one standard deviation to the reported emissions. The error bars only represent the variation in the flux measurements and not the uncertainty in measurements or in reported emissions. The *x* scale only indicates the year of the measurements; the *x* position within a year has no meaning. Reported emissions for 2011 were used for the 2012 ratios since 2012 data were not yet available.

Since the Longview study in 2012 was focused on only a single industrial complex, an unusually large number of measurements were performed. In total, 67 measurements of ethene emissions, 60 of propene emissions, and 92 of NO_2 emissions were performed on 8 different days in a 9 day period. This gives a fairly detailed picture of how much total emissions from an industry varies during a week. The histograms in Figure 12 show the distribution of fluxes for all measurements of these three species. During the measurement period, two episodes with atypical emissions were identified. On the afternoon of May 7, ethene emissions were significantly elevated after having been at more typical levels earlier in the day. Similarly, propene emissions were elevated during May 10. These elevated emissions were suspected to be due to upsets or irregular operation. The measurements from these episodes are shown separately in the histograms in Figure 12. Excluding these two episodes, the variability of the measured fluxes is fairly small for all three species. For ethene the average emission of all SOF transects is 205 ± 57 kg/h, excluding the presumed upset. Similarly, the average propene emission is 172 ± 77 kg/h without presumed upset emissions. No upset episodes were identified for the NO_2 emissions. The average NO_2 emission during the whole study was 118 ± 33 kg/h. The flux distributions for ethene and NO_2, with the identified upset for ethene excluded, are approximately Gaussian in shape with standard deviations of about 30% of the mean. Measurement variability of this magnitude is often intrinsic to local wind field variability not captured by the wind measurements and not necessarily indicative of the true emission variability. The propene flux distribution, on the other hand, is a bit more irregular with larger variability, even after excluding the identified upset episode. This is probably more than can be explained by wind variability alone, indicating that propene emissions were less constant during the period, although still relatively stable. This study suggests that apart from isolated upset episodes, the total emissions from a petrochemical complex like this is fairly stable on the time scale of slightly more than a week. The average emissions for all transects, including the upset episodes, were 249 ± 130 kg/h for ethene and 211 ± 122 kg/h for propene, which is 21% and 22% higher than without the upset episodes. This is only a single site and a fairly limited period, but if it is taken to be representative of typical conditions, it would indicate that nonroutine emissions account for a relatively small part of total annual emissions, even though they can dominate the momentaneous emissions at times. This conclusion is also compatible with the broad patterns of the measurements in other areas presented in this study, even though the lower number of measurements in those areas makes it more difficult to clearly separate routine emissions from upset events. A notable example to this pattern, however, is the 2006 propene measurement in the HSC, which indicated huge variations in emissions over short time periods. This may, however, have been a rare event, since nothing similar has been seen after that.

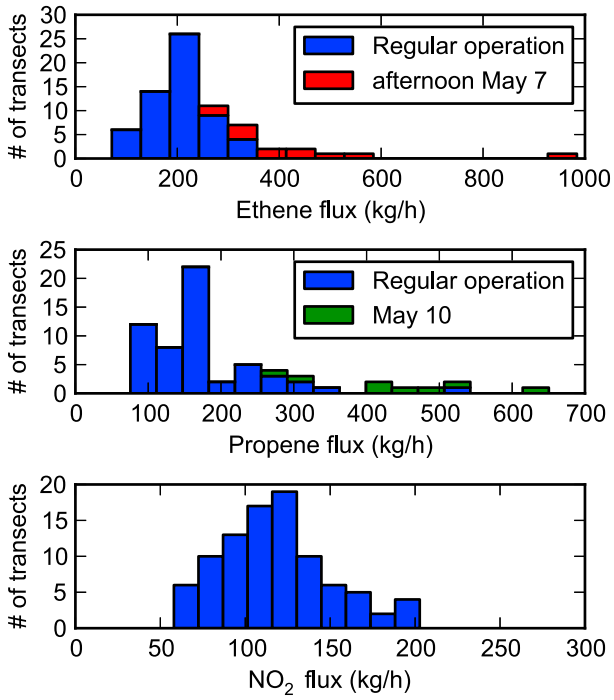

Figure 12. Histograms showing the distribution of all flux measurements of ethene, propene, and NO_2 during 2012. Ethene emissions were significantly elevated during the afternoon on 7 May, and similarly, propene emissions were higher than usual on 10 May. Fluxes measured during these episodes are plotted as separated additive histograms.

4. Discussion

4.1. Measurement Uncertainty

The main uncertainty associated with SOF and mobile DOAS flux measurements generally comes from the uncertainty in the wind field. Uncertainties for the measured wind speeds and wind directions were estimated from comparisons of wind profile averages to normalized ground wind measurements. The estimated uncertainties are given in Table 2. Since the calculated flux is proportional to the wind speed, the uncertainty of the wind speed carries over to the flux proportionally. For the wind direction uncertainty, however, the impact on the flux is not linear and also depends on how orthogonal the measurement transect is to the wind direction. To estimate the flux uncertainty due to wind direction uncertainty, measurement situations were simulated with wind errors drawn from a normal distribution based on the estimated wind direction uncertainties, and the average absolute flux error was calculated from a large number of simulations. This was done for 90° and 75° angles between the transect and wind direction to represent the typical range of measurement scenarios and for the estimated wind direction uncertainties of all four studies. The results are given in Table 5. This uncertainty estimate is somewhat conservative, since large wind direction errors can usually be avoided by estimating the wind direction from geometric constraints, i.e., the approximate locations of the sources and where the plume was detected. For the 2012 study, the comparisons of wind profile averages to normalized ground wind measurements gave unusually large wind direction uncertainty estimates, but the simple measurement geometry with only one large industrial complex enabled the actual wind direction uncertainty to be significantly limited by geometrical constraints. To avoid a needlessly conservative uncertainty estimate in this case, wind errors were restricted to a maximum of ±15° in the simulations for this study.

The cross-section uncertainties are generally well established by the experimentalists who have measured them. The infrared cross sections for the VOCs have an uncertainty of 3–3.5% [*Sharpe et al*., 2004], while the UV cross sections have uncertainties of 2.8% for SO_2 [*Bogumil et al*., 2003] and 4% for NO_2 [*Vandaele et al*., 1998]. Additionally, retrieval errors of 10–20% have been estimated for the different species. This is the combined effect of instrument and retrieval stability on the total columns for a plume transect [*Mellqvist et al*., 2010b]. For the alkane retrieval this also includes the 6% mass retrieval uncertainty established above. All these uncertainty sources have been combined by root-sum-square to a composite flux measurement

Table 5. Error Budget for the Flux Measurements During the Different Studies[a]

			Alkanes	Ethene	Propene	SO_2	NO_2
Cross-Section Uncertainty			3.5%	3.5%	3.5%	2.8%	4%
Retrieval Error			12%	10%	10%, 20%	10%	10%
Year	Wind Speed	Wind Direction	Composite Flux Measurement Uncertainty				
2006	15–27%	8–12%	21–32%	20–31%	26–36%	20–31%	20–31%
2009	11–29%	7–10%	18–33%	17–32%	24–37%	17–32%	17–33%
2011	16–30%	5–8%	21–33%	20–33%	26–37%	20–33%	20–33%
2012	25–34%	4–12%	28–38%	27–38%	32–41%	27–38%	28–38%

[a]The cross-section uncertainties and estimated retrieval errors depend mainly on the species, while the wind speed and wind direction errors have been estimated separately for each year but apply equally to all species. These four error sources are combined by root-sum-square to a composite flux measurement uncertainty for each species and year. The highest and lowest composite uncertainties in the ranges given were calculated using the lowest and highest uncertainties for both wind speed and direction.

uncertainty range for each species and study. The maximum and minimum for each range were calculated using the maximum and minimum uncertainties of both wind speed and wind direction. These are given in Table 5. In most cases, the composite uncertainty is approximately 20–35%. The high retrieval error estimated for propene (20%) was due to instrumental problems that were primarily present during the 2009 and 2011 studies. These problems primarily affected measurements of small propene columns. Many of the propene measurements actually had a lower retrieval error than this, but 20% was used in the composite errors in Table 5.

4.2. Representativeness of Measurements

In Table 4 and Figure 11, the results of the SOF and mobile DOAS measurements are compared to reported annual average emissions. The relevance of this comparison depends on whether measurements during shorter periods, a few weeks in these cases, can be expected to be representative for the average emissions over a full year. One argument against this is that temporary emissions or upsets, which only last a limited time period, may be overrepresented in the SOF measurements. Examples of this include emissions occurring during tank cleaning operations, ship loading, flaring, and accidental releases. This type of events occurs rather frequently and might typically last for 1–24 h. Hence, it is likely that some of the SOF measurements include emissions from such events. This type of event is likely to be the explanation for upset emission identified in the Longview measurements in 2012, as illustrated in Figure 12. This example showed that it is possible to discriminate between such upsets and average emissions if a large number of measurements are performed but that the influence of the upset emissions was relatively small on the estimated average emissions.

The industrial areas studied in this paper consist of a large number of independent sites, especially the HSC, and short-term upsets should occur in at least some of the sites during each transect. On the other hand, it is unlikely that they occur in a large fraction of them at the same time, and hence the relative elevation of the total emissions from all of them will be much smaller than for the sites where the upset occurs. The fact that the emissions, for instance, of alkanes from the HSC, show relatively small variations from transect to transect and over several years, as shown in Table 4, indicates that the SOF measurements are representative for long time periods and that the impact of longer term upset emissions is averaged out. On the other hand, this was not the case for the 2006 propene measurements in the HSC, where the emission showed large temporal variability that was attributed to flaring activity in petrochemical plants [*Mellqvist et al*., 2010b]. These emissions decreased in the later years and have since been more stable. This shows that upsets can have a significant impact on total emissions in some cases and that measurements over longer periods or repeated studies over several years might be needed to make such distinctions.

Another potential reason why the measurements presented in this paper might not be representative for the annual average emissions is that there might be systematic differences in meteorological conditions between the measurement periods and the whole years that could have a large effect on the emission rates of some facilities. All four studies were conducted during the warmer half of the year, during daytime and in clear conditions. All these factors would be expected to contribute to higher than average ambient temperature and solar insolation. Wind speeds might also have been unrepresentative during the studies, which might have caused higher than average emissions. The emission sources most sensitive to meteorological conditions are probably storage tanks for crude oil and for refined products. Ambient temperature and solar

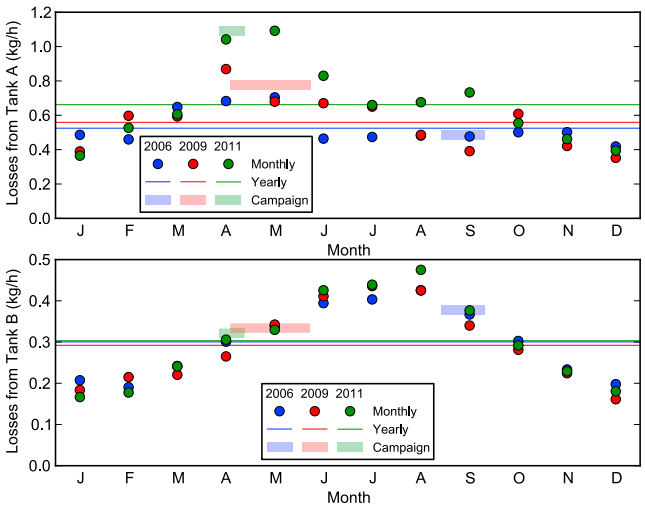

Figure 13. Emission rates from Tank A (external floating roof tank with crude oil) and Tank B (internal floating roof tank with gasoline) calculated using emission factor formulas and meteorological data averaged over different time periods. Circles indicate emissions calculated using monthly averages, and bars indicate emissions calculated using averages over the campaign periods, as well as the extent of these campaigns. Yearly averages of the monthly emissions were calculated and indicated with horizontal lines.

insolation affect the liquid surface temperature of the product in tanks which in turn affect the vapor pressure and thereby evaporation. Wind speed primarily affects losses in external floating roof tanks. Ethene, propene, and other products that are gaseous under ambient conditions are stored in pressurized tanks, which should not be expected to have losses significantly affected by meteorology. Temperatures and pressures of feedstocks and products in process steps are typically monitored and regulated and thereby not significantly affected by ambient conditions. Effects of ambient temperatures, solar radiation, and wind speed are included in the formulas for estimation of storage tank losses in *AP-42*, *Compilation of Air Pollutant Emission Factors* [*USEPA*, 2013], EPA's primary compilation of emission factor information, which most emission estimates reported to the emission inventories are based on. To estimate the effects of the differences in meteorological conditions, the campaign periods, and the entire years, formulas from *AP-42* were used to estimate the emissions from an external floating roof tank storing crude oil (Tank A) and from an internal floating roof tank storing gasoline (Tank B). These were chosen to represent the most typical tanks with significantly meteorology-affected emissions. Emissions from these tanks were estimated on a monthly basis using monthly averages of the hourly meteorology data. The meteorological data consisted of measurements of ambient temperature, solar radiation and wind speed from the TCEQ monitoring station C1015 [*TCEQ*, 2013]. Annual average emissions were calculated as the average of monthly emissions for all months in each year. Average emissions during each campaign were calculated using averages of the meteorological data for the duration of the campaign. Figure 13 shows the effects of using meteorological data from these different periods in 2006, 2009, and 2011 on calculated emissions from Tank A and Tank B. Meteorological data were missing from C1015 for October and November 2011, so average values for the same months in 2006 and 2009 were used instead. For Tank B the intrayear variations in emissions are quite similar from year to year, while for Tank A there are larger differences between the years, and especially 2011 stands out. The reason for this is that, according to the AP-42 emission factors, emissions from external floating roof tanks are sensitive to wind speed, while emissions from internal floating roof tanks are unaffected by wind. During the summer half of 2011, winds speeds were significantly higher than during the same periods in 2006 and 2009, especially in April and May. For this reason, the calculated emissions from Tank A for the campaign period were approximately 65% higher than the annual average, while for 2009 it was only 39% higher and for 2006 it was 8% lower. For Tank B the corresponding differences were smaller: 26%, 14%, and 6% higher during the campaign periods in 2006, 2009, and 2011, respectively.

The differences in calculated emissions presented in Figure 13 are only the seasonal variations. There are of course also day-to-day variations and differences between daytime and nighttime. Assessing these variations

Table 6. Average Temperatures, Solar Radiations, and Wind Speeds During the Whole Campaigns Compared to Daytime (9–18) on the SOF-Measurement Days and the Estimated Effects of These Differences in Meteorology on Tank Emissions of Alkanes From an External Floating Roof Tank Storing Crude Oil (A) and From an Internal Floating Roof Tank Storing Gasoline (B)[a]

Year	Tank	Mean Temperature Campaign (°C)	Mean Temperature Measurement Days (°C)	Effect of Temperature Difference on Emissions	Mean Solar Radiation Campaign (W/m^2)	Mean Solar Radiation Measurement Days (W/m^2)	Effect of Solar Radiation Difference on Emissions	Mean Wind Speed Campaign (m/s)	Mean Wind Speed Measurement Days (m/s)	Effect of Wind Speed Difference on Emissions	Combined Effect on Emissions	Difference Between Campaign and Year	Total Difference Between Measurement Days and Year
2006	A	27.3	26.5	−2.2%	208	677	8.3%	3.8	4.8	40.3%	49.0%	−7.9%	37.2%
	B			−4.2%			17.0%			0.0%	11.5%	25.5%	39.9%
2009	A	24.9	26.3	4.6%	248	712	8.9%	5.4	4.9	−14.2%	−2.5%	39.2%	35.7%
	B			7.8%			15.5%			0.0%	25.4%	14.3%	43.3%
2011	A	24.2	26.1	6.7%	232	649	8.2%	7	7.5	0.0%	15.6%	64.5%	90.2%
	B			10.8%			13.5%			0.0%	26.7%	6.0%	34.3%

[a]Combined with the effect of whole campaign averages versus annual averages (as shown in Figure 13), the total elevation of alkane emissions due to the meteorological conditions during the measurements is estimated.

using the *AP-42* formulas requires applying the formulas on time scales of single days or even hours or at least to averages of meteorological from nonconsecutive time periods on such scales. This is not how the formulas in *AP-42* are typically applied and not what they were designed for. Instead, emissions are typically calculated using monthly or even annual averages. Since the campaign periods were of similar time scales as months, the campaign averages in Figure 13 are probably comparable to monthly averages. To estimate the variations on shorter time scales, the *AP-42* formulas have been applied to averages of meteorological data from daytime hours (9:00–18:00 CDT) on the days in each campaign when SOF measurements were made. Applying the formulas in this way is likely to give overestimated differences compared to averages for the whole campaign, primarily because the surface temperature in a tank might not follow changes in ambient temperature and solar radiation on the scale of hours or days in the same way as it does on the time scale of months or years. There might be memory effects from the ambient temperatures and solar radiation in previous hours or days, which are likely to be averaged out over a month. The differences given by applying the formulas like this can, however, be thought of as upper estimates of actual differences. Table 6 shows the differences between the daytime averages of the SOF measurement days and whole campaign averages for ambient temperature, solar radiation, and wind speed, and the differences to the calculated emissions from Tank A and Tank B from using averages of measurement days instead of campaign averages. These effects are shown for each meteorological parameter separately as well as the combined effect. Additionally, the last two columns show the differences between campaign averages and annual averages (as shown in Figure 13), as well as the total effect of both seasonal and shorter term variations. The total effect typically adds up to 35–45% for both tanks, with the exception of Tank A in 2011. This exceptionally large effect was due to the strong winds during the campaign. The winds were so strong that the campaign average was outside the applicable range of the *AP-42* formulas, 0–15 mph, and hence there was no extra effect due to the short-term variations.

The calculated total effects should be considered as upper estimates, since they assume that there are no memory effects from the cooler nighttime conditions suppressing the daytime emissions. Assuming that storage tanks represent roughly two thirds of the emissions from typical refineries [*Kihlman*, 2005] and that emissions from process steps are not significantly affected by meteorological conditions, the total meteorological effects estimated above indicate that the alkane emissions measured from refineries in this paper may be 20–30% higher than the annual average.

Neither meteorological effects nor elevated emissions due to upset events seem to be even close in magnitude to the discrepancies between measurements and emission inventories, and hence these discrepancies most likely represent an underestimation of the continuous routine emissions by the inventories.

5. Conclusions

Total emissions of alkanes, ethene, propene, SO_2, and NO_2 from a number of large industrial areas dominated by refineries and petrochemical industries were measured during four measurement campaigns in the period 2006–2012. The measurement error analysis indicates uncertainties typical within 20–35%. In comparison to annual average emissions reported to emission inventories, the VOCs (alkanes, ethene, and propene) stood out with measured emissions typically exceeding reported emissions by factor of 5–15, while measured SO_2 and NO_2 emissions were much closer to reported emissions. A tank model analysis of the effect of wind speed, solar radiation, and ambient temperature on tank emissions shows that the alkane emissions measured from tanks in this study may have been up to 35–45% higher than the annual average, and in 2011 that effect may have been even larger for crude oil tanks due to exceptionally strong winds. These meteorological effects are not nearly large enough to explain the discrepancies between SOF measurements and emission inventories, and they are also not applicable to process emissions and alkene emissions from petrochemical industries. A detailed study of alkene emissions from a petrochemical complex in Longview indicated that upset emissions can cause an increase in total emissions on the order of 20% compared to the continuous routine emissions. Upset emissions are of course highly irregular by nature, but the relatively limited variation in the other VOC emission measurements presented confirms the notion that total emissions are typically dominated by routine emissions rather than by upset emissions.

Since neither upset emissions nor meteorological effects can account for the large emission discrepancies, the conclusion from these results is that current emission inventories, based on emission factor calculations, systematically fail to quantify continuous industrial VOC emissions and that reliable estimates of these emissions can currently only be obtained from measurements.

Acknowledgments

The 2006 study was funded by Houston Advanced Research Center (HARC) under project H53. The 2009 study was funded by Texas Environmental Research Consortium (TERC) under project H102. The 2011 study was funded by the state of Texas through the Air Quality Research program administered by the University of Austin under project 10-006. The 2012 study was funded by the state of Texas through the East Texas Council of Governments (ETCOG) under the technical direction of Northeast Texas Air Care (NETAC). The additional data analysis and writing of this paper was funded by TCEQ under a separate project. The authors would like to thank TCEQ for supplying wind data and John Jolly at TCEQ for supplying data from the STARS (State of Texas Air Reporting System) emission inventory.

References

Angelbratt, J., et al. (2011), A new method to detect long term trends of methane (CH_4) and nitrous oxide (N_2O) total columns measured within the NDACC ground-based high resolution solar FTIR network, *Atmos. Chem. Phys.*, *11*(13), 6167–6183, doi:10.5194/acp-11-6167-2011.

Berg, N., J. Mellqvist, J. P. Jalkanen, and J. Balzani (2012), Ship emissions of SO_2 and NO_2: DOAS measurements from airborne platforms, *Atmos. Meas. Tech.*, *5*(5), 1085–1098, doi:10.5194/amt-5-1085-2012.

Bogumil, K., et al. (2003), Measurements of molecular absorption spectra with the SCIAMACHY pre-flight model: Instrument characterization and reference data for atmospheric remote-sensing in the 230–2380 nm region, *J. Photochem. Photobiol., A*, *157*(2–3), 167–184, doi:10.1016/S1010-6030(03)00062-5.

Burrows, J. P., A. Richter, A. Dehn, B. Deters, S. Himmelmann, S. Voigt, and J. Orphal (1999), Atmospheric remote-sensing reference data from GOME—2. Temperature-dependent absorption cross sections of O3 in the 231-794 nm range, *J. Quant. Spectros. Radiat. Transfer*, *61*(4), 509–517.

Cantrell, C. A., J. A. Davidson, A. H. McDaniel, R. E. Shetter, and J. G. Calvert (1990), Temperature-dependent formaldehyde cross sections in the near-ultraviolet spectral region, *J. Phys. Chem.*, *94*(10), 3902–3908.

De Gouw, J. A., et al. (2009), Airborne measurements of ethene from industrial sources using laser photo-acoustic spectroscopy, *Environ. Sci. Technol.*, *43*(7), 2437–2442, doi:10.1021/es802701a.

Fayt, C. (2011), QDOAS 1.00, edited, Belgian Institute for Space Aeronomy, Brussles, Belgium.

Galle, B., C. Oppenheimer, A. Geyer, A. J. S. McGonigle, M. Edmonds, and L. Horrocks (2002), A miniaturised ultraviolet spectrometer for remote sensing of SO_2 fluxes: A new tool for volcano surveillance, *J. Volcanol. Geotherm. Res.*, *119*(1–4), 241–254, doi:10.1016/S0377-0273(02)00356-6.

Gilman, J. B., et al. (2009), Measurements of volatile organic compounds during the 2006 TexAQS/GoMACCS campaign: Industrial influences, regional characteristics, and diurnal dependencies of the OH reactivity, *J. Geophys. Res.*, *114,* D00F06, doi:10.1029/2008JD011525.

Hermans, C., A. C. Vandaele, M. Carleer, S. Fally, R. Colin, A. Jenouvrier, B. Coquart, and M. F. Mérienne (1999), Absorption cross-sections of atmospheric constituents: NO_2, O_2, and H_2O, *Environ. Sci. Pollut. Res.*, *6*(3), 151–158.

Jobson, B. T., C. M. Berkowitz, W. C. Kuster, P. D. Goldan, E. J. Williams, F. C. Fesenfeld, E. C. Apel, T. Karl, W. A. Lonneman, and D. Riemer (2004), Hydrocarbon source signatures in Houston, Texas: Influence of the petrochemical industry, *J. Geophys. Res.*, *109*, D24305, doi:10.1029/2004JD004887.

Johansson, J. K. E., J. Mellqvist, J. Samuelsson, B. Offerle, B. Rappenglück, D. Anderson, B. Lefer, S. Alvarez, and J. Flynn (2011), Quantification of industrial emissions of VOCs, NO_2 and SO_2 by SOF and Mobile DOAS, *Rep. 10-006*, AQRP.

Johansson, J. K. E., J. Mellqvist, B. Lefer, and J. Flynn (2012), SOF HRVOC emission study at Longview, Texas, *Rep.*, ETCOG.

Johansson, J. K. E., J. Mellqvist, J. Samuelsson, B. Offerle, J. Moldanova, B. Rappenglück, B. Lefer, and J. Flynn (2014), Quantitative measurements and modeling of industrial formaldehyde emissions in the Greater Houston area during campaigns in 2009 and 2011, *J. Geophys. Res. Atmos.*, doi:10.1002/2013JD020159.

Johansson, M., B. Galle, T. Yu, L. Tang, D. Chen, H. Li, J. X. Li, and Y. Zhang (2008), Quantification of total emission of air pollutants from Beijing using mobile mini-DOAS, *Atmos. Environ.*, *42*(29), 6926–6933, doi:10.1016/j.atmosenv.2008.05.025.

Johansson, M., C. Rivera, B. DeFoy, W. Lei, J. Song, Y. Zhang, B. Galle, and L. Molina (2009), Mobile mini-DOAS measurement of the outflow of NO_2 and HCHO from Mexico City, *Atmos. Chem. Phys.*, *9*(15), 5647–5653, doi:10.1029/2005GL022616.

Karl, T., T. Jobson, W. C. Kuster, E. Williams, J. Stutz, R. Shetter, S. R. Hall, P. Goldan, F. Fehsenfeld, and W. Lindinger (2003), Use of proton-transfer-reaction mass spectrometry to characterize volatile organic compound sources at the La Porte super site during the Texas Air Quality Study 2000, *J. Geophys. Res.*, *108*(16), 4508, doi:10.1029/2002JD002967.

Kihlman, M. (2005), Application of Solar FTIR spectroscopy for quantifying gas emissions, Chalmers Univeristy of Technology.

Kim, S. W., et al. (2011), Evaluations of NO_x and highly reactive VOC emission inventories in Texas and their implications for ozone plume simulations during the Texas Air Quality Study 2006, *Atmos. Chem. Phys.*, *11*(22), 11,361–11,386, doi:10.5194/acp-11-11361-2011.

Kleinman, L. I., P. H. Daum, D. Imre, Y. N. Lee, L. J. Nunnermacker, S. R. Springston, J. Weinstein-Lloyd, and J. Rudolph (2002), Ozone production rate and hydrocarbon reactivity in 5 urban areas: A cause of high ozone concentration in Houston, *Geophys. Res. Lett.*, *29*(10), 1467, doi:10.1029/2001GL014569.

Lefer, B. (2009), Study of Houston Atmospheric Radical Precursors (SHARP), *Rep.*, University of Houston.

Mellqvist, J., J. Samuelsson, C. Rivera, B. Lefer, and M. Patel (2007), Measurements of industrial emissions of VOCs, NH_3, NO_2 and SO_2 in Texas using the Solar Occultation Flux method and mobile DOAS, *Rep.*, HARC.

Mellqvist, J., J. K. E. Johansson, J. Samuelsson, B. Offerle, B. Rappenglück, C.-S. Wilmot, and R. Fuller (2010a), Investigation of VOC radical sources in the Houston area by the Solar Occultation Flux (SOF) method, mobile DOAS (SOF-II) and mobile extractive FTIR, *Rep.*, TERC.

Mellqvist, J., J. Samuelsson, J. K. E. Johansson, C. Rivera, B. Lefer, S. Alvarez, and J. Jolly (2010b), Measurements of industrial emissions of alkenes in Texas using the solar occultation flux method, *J. Geophys. Res.*, *115*, D00F17, doi:10.1029/2008JD011682.

Parrish, D. D., et al. (2009), Overview of the second Texas air quality study (TexAQS II) and the Gulf of Mexico atmospheric composition and climate study (GoMACCS), *J. Geophys. Res.*, *114*, D00F13, doi:10.1029/2009JD011842.

Rivera, C., G. Sosa, H. Wöhrnschimmel, B. De Foy, M. Johansson, and B. Galle (2009), Tula industrial complex (Mexico) emissions of SO_2 and NO_2 during the MCMA 2006 field campaign using a mobile mini-DOAS system, *Atmos. Chem. Phys.*, *9*(17), 6351–6361, doi:10.1029/2002GL015827.

Rivera, C., J. Mellqvist, J. Samuelsson, B. Lefer, S. Alvarez, and M. R. Patel (2010), Quantification of NO_2 and SO_2 emissions from the Houston Ship Channel and Texas City industrial areas during the 2006 Texas Air Quality Study, *J. Geophys. Res.*, *115*, D08301, doi:10.1029/2009JD012675.

Rothman, L. S., et al. (2005), The HITRAN 2004 molecular spectroscopic database, *J. Quant. Spectros. Radiat. Transfer*, *96*(2), 139–204, doi:10.1016/j.jqsrt.2004.10.008.

Ryerson, T. B., et al. (2003), Effect of petrochemical industrial emissions of reactive alkenes and NO_x on tropospheric ozone formation in Houston, Texas, *J. Geophys. Res.*, *108*(8), 4249, doi:10.1029/2002JD002746.

Sharpe, S. W., T. J. Johnson, R. L. Sams, P. M. Chu, G. C. Rhoderick, and P. A. Johnson (2004), Gas-phase databases for quantitative infrared spectroscopy, *Appl. Spectrosc.*, *58*(12), 1452–1461, doi:10.1366/0003702042641281.

Stutz, J., O. Pikelnaya, G. Mount, E. Spinei, S. C. Herndon, E. C. Wood, O. Oluwole, W. Vizuette, and E. Causo (2011), Quantification of hydrocarbon, NO_x, and SO_2 emissions from petrochemical facilities in Houston: Interpretation of the 2009 FLAIR dataset, *Rep. 10-045*, AQRP.

Texas Commission on Environmental Quality (TCEQ) (2013), Data from Continuous Ambient Monitoring Stations, edited by TCEQ.

United States Environmental Protection Agency (USEPA) (2013), AP-42, Compilation of Air Pollutant Emission Factors, Fifth ed.

Vandaele, A. C., C. Hermans, P. C. Simon, M. Carleer, R. Colin, S. Fally, M. F. Mérienne, A. Jenouvrier, and B. Coquart (1998), Measurements of the NO_2 absorption cross-section from 42 000 cm^{-1} to 10 000 cm^{-1} (238–1000 nm) at 220 K and 294 K, *J. Quant. Spectros. Radiat. Transfer*, *59*(3–5), 171–184.

Washenfelder, R. A., et al. (2010), Characterization of NO_x, SO_2, ethene, and propene from industrial emission sources in Houston, Texas, *J. Geophys. Res.*, *115*, D16311, doi:10.1029/2009JD013645.

Wert, B. P., et al. (2003), Signatures of terminal alkene oxidation in airborne formaldehyde measurements during TexAQS 2000, *J. Geophys. Res.*, *108*(3), 4104, doi:10.1029/2002JD002746.